Protection against Chemical and Biological Threats Using Metal-Organic Frameworks as Active Layers

Kaikai Ma, [*,†,#] Yuk Ha Cheung,[‡,#] Kent O. Kirlikovali,[†,#] Xiaoliang Wang,[†] Timur Islamoglu,[†] John Xin,[‡] and Omar K. Farha[*,†,⊥]

[†]International Institute for Nanotechnology, Institute for Sustainability and Energy at Northwestern, and Department of Chemistry, Northwestern University, 2145 Sheridan Road, Evanston, Illinois 60208, United States

[‡]Research Centre for Smart Wearable Technology, School of Fashion and Textiles, The Hong Kong Polytechnic University, Kowloon 999077, Hong Kong SAR

[⊥]Department of Chemical and Biological Engineering, Northwestern University, 2145 Sheridan Road, Evanston, Illinois 60208, United States

The SARS-CoV-2 pandemic outbreak and the unfortunate misuse of toxic chemical warfare agents (CWAs) highlight the importance of developing functional materials to protect against these chemical and pathogen threats. Metal–organic frameworks (MOFs), which comprise a tunable class of crystalline porous materials built from inorganic nodes and organic linkers, have emerged as a class of heterogeneous catalysts capable of rapidly detoxify multiple classes of these harmful chemical or biological hazards. In particular, zirconium-based MOFs (Zr-MOFs) feature Lewis acidic nodes that serve as active sites for a wide range of catalytic reactions, including the hydrolysis of organophosphorus nerve agents within seconds in basic aqueous solutions. In addition, post-synthetic modification of Zr-MOFs enables the release of active species capable of reacting with and deactivating harmful pathogens. Despite this impressive performance, utilizing Zr-MOFs in powder form is not practical for application in masks or protective uniforms.

To address this challenge, our team sought to develop MOF/fiber composite systems that could be adapted for use under realistic operating conditions to protect civilians, military personnel, and first responders from harmful pathogens and chemical warfare agents. Over the last several years, our group has designed and fabricated reactive and biocidal MOF/fiber composites that effectively capture and deactivate these toxic species. In this Account, we describe the evolution of these porous and reactive MOF/fiber composites and focus on key design challenges and considerations.

First, we devised a scalable method for the integration of Zr-MOFs onto textile substrates using aqueous precursor solutions and without using pre-treated textiles, highlighting the potential scalability of this method. Moving beyond standard textiles, we also developed a microbial synthesis strategy to prepare hierarchically porous

MOF/bacterial cellulose nanofiber composite sponges that can both capture and detoxify nerve agents when exposed to contaminated gas flows. Next, we demonstrated that heterogeneous polymeric bases are suitable replacements for volatile liquid bases typically used in solution-phase reactions, and we showed that these composite systems are capable of effectively hydrolyzing nerve agents in solid-state by using only water that is present as humidity. Moreover, incorporating a reactive dye precursor into the composite affords a dual function sensing and detoxifying material that changes color from white to orange upon reaction with the byproduct following nerve agent hydrolysis, demonstrating the versatility of this platform for use in decontamination applications. We then created chlorine-loaded MOF/fiber composites that act as biocidal and reactive textiles that are capable of not only detoxifying sulfur mustard-based chemical warfare agents and simulants, but also deactivating both bacteria and the SARS-CoV-2 virus within minutes of exposure. Finally, we synthesized a mixed-metal Ti/Zr-MOF coating on cotton fibers to afford a photoactive biocidal cloth that shows fast and broad-spectrum biocidal performance against viruses and Gram-positive and Gram-negative bacteria under visible light irradiation.

Given the tunable, multi-functional nature of these MOF/fiber composites, we believe that this Account will offer new insights for the rational design and preparation of functional MOF/fiber composites and pave the way towards the development of next-generation reactive and protective textiles.

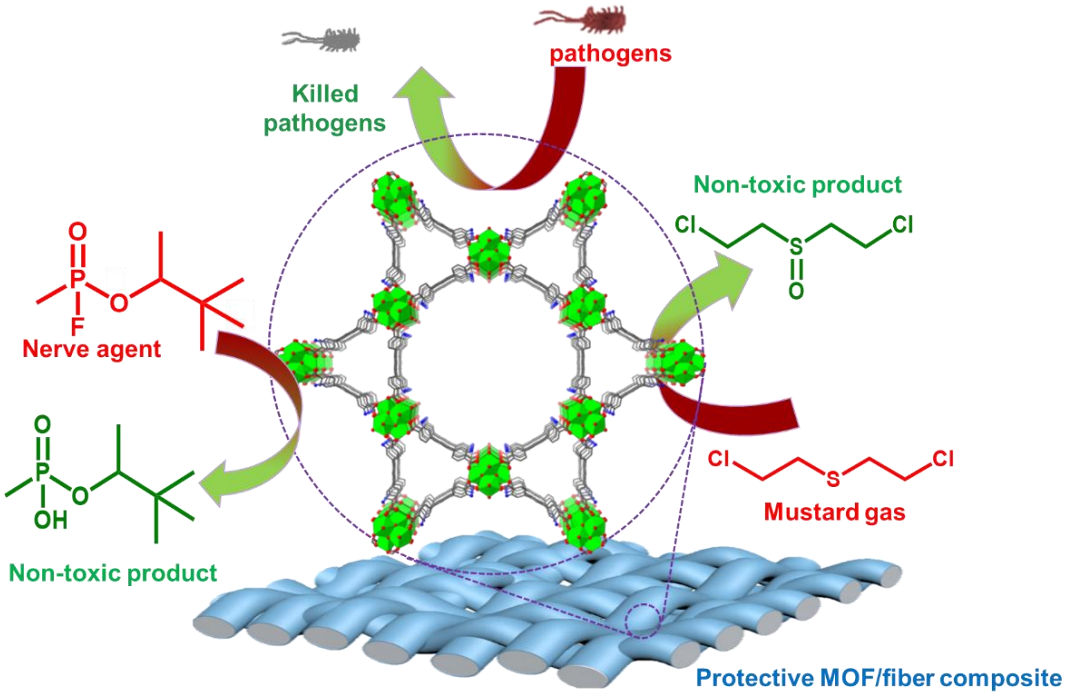

Figure 1. Schematic illustration of protective MOF/fiber composite against

chemical and biological risks.

Introduction

Across civilian healthcare and military fields, protective clothing and masks provide critical protection means biological and chemical threats, such as the SARS-CoV-2 virus and chemical warfare agents (CWAs), respectively.[1-9] Rather than degrade or deactivate these threats, traditional fibrous protective clothing and masks only block or delay penetration of these molecules, resulting in the need for thick protective layers that limit dexterity and breathability for the user.[1-9] Moreover, viruses and bacteria have been detected on surfaces in healthcare settings days after contamination, and CWAs are chemically stable with half-lives ranging from days to weeks, highlighting the long-term exposure risk for humans and complicating the safe disposal of these materials after each exposure.[10-13] As a result, the development of self-cleaning protective textile materials has become increasingly important within recent years, especially considering the COVID-19 pandemic caused by the SARS-CoV-2 virus and the continued, recent use of CWAs against civillians.[1-2]

Metal-organic frameworks (MOFs), a highly tunable class of porous crystalline solids constructed from metal-based nodes and organic linkers,[14-19] comprise a platform that has great potential in protective applications, including elimination of CWAs and pathogens.[20-44] However, MOFs are generally isolated from production as powders, which are poorly processable and limit the potential use of these materials as protective layers. Therefore, the crucial step toward the realization of MOFs in protective masks and clothes involves the integration of functional MOF particles into flexible fibrous substrates.[1-2,29-44] Over the last decade, researchers have explored various routes to fabricate MOF/fiber composites and explored their use in CWA detoxification applications and towards the deactivation of harmful bacteria and viruses (Figure 1).[1-2,31-44] In this Account, we present our group's progress in this area, starting with strategies to design and synthesize robust MOF/fiber composites and moving towards the application of these composites as protective materials against chemical and biological threats.

1. Synthetic routes to produce MOF/fiber composites

While powdered MOFs exhibit excellent activity in the solution-state catalytic degradation of CWAs, the poor processability of powdered MOFs hinders the use of these MOF catalysts in practical, fully solid-state applications. Therefore, the fabrication of MOF/fiber composites is critical for realizing the potential of MOFs in chemical and biological protective gear.[33,35] Two of the most common strategies for the synthesis of MOF/fiber composites involve either the *in situ* growth of the MOF coating

onto the fiber, or the incorporation of preformed MOF particles onto fiber. Below, we describe our recent progress on the synthesis of MOF/fiber composites using these two strategies, including the *in situ* hydrothermal growth of MOF layers on fiber surfaces[37-38] and a dip-coating method using Zr-MOF nanoparticles,[39-41] as well as a bio-synthesis method that starts with Zr-MOF nanoparticles and generates a cellular nanofiber network through fermentation.[42] In all cases, the MOF imparts desired functionality and reactivity to the composite, while the fiber substrate endows the MOF-containing composite with excellent processability and flexibility.

1.1. *In situ* hydrothermal growth

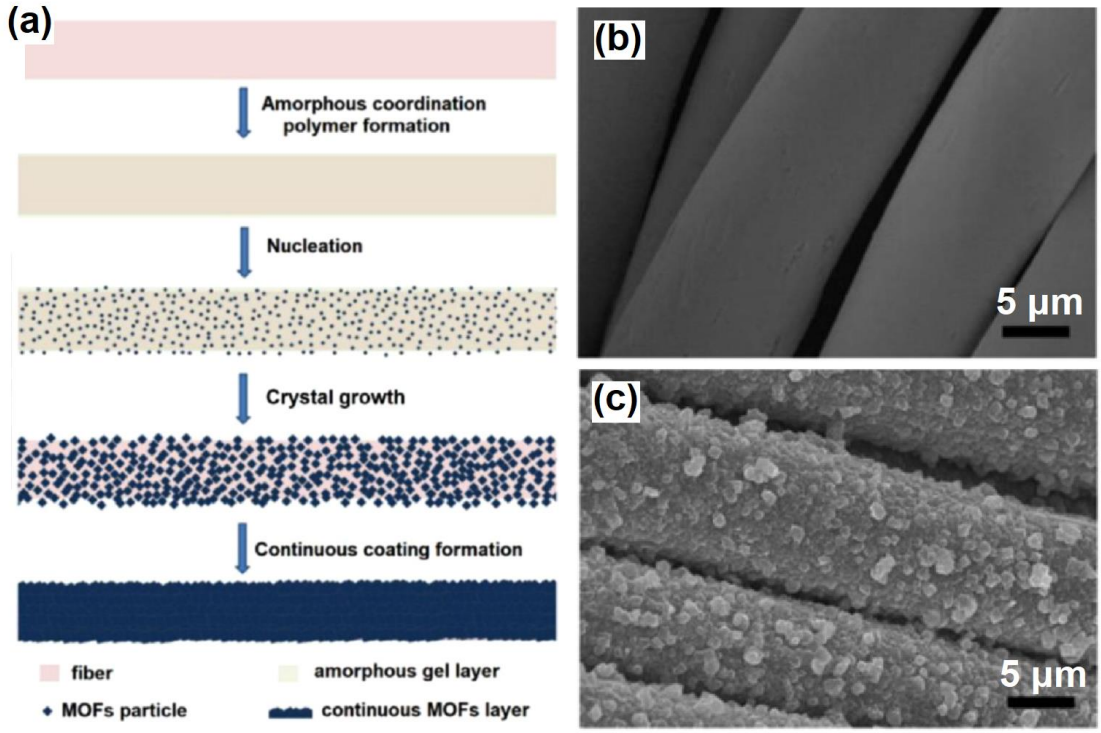

Figure 2. (a) Schematic illustration of the template-free aqueous synthesis of Zr-MOF coatings on fiber. SEM images of (b) the PET fiber and (c) the prepared MOF-808/PET sample. Adapted from ref (37). Copyright 2019 American Chemical Society.

In the *in situ* solvothermal growth method, the reaction vessel contains a swatch of fiber immersed in a solution of the MOF precursors (i.e., metal salt and organic linker), and it is heated for a set amount of time to form a MOF layer directly on the fiber surface. However, researchers must address several practical challenges when employing this approach. Generally, most textile fiber surfaces are chemically inert and unfavorable for the nucleation and growth of MOF particles. As a result, most of the widely used solvothermal methods afford low efficiencies in coating MOFs on fiber substrates, and these strategies yield relatively more MOF particles in the reaction media relative to

the amount coated onto the fiber surfaces.[36,37] Although chemically modifying the textile support with reactive groups that can coordinate to the metal nodes promotes MOF nucleation on the fiber, this strategy increases the process complexity and the cost and may present future challenges during the scale up of these strategies. In addition, most reported solvothermal strategies require the use of toxic solvents during the composite synthesis, such as *N,N*-dimethylformamide (DMF), which can potentially dissolve/destroy many commonly used fibers at high temperatures required for MOF synthesis.[37] Even if the fiber is compatible with these harsh conditions, trapped solvent molecules in the composite pose a potential threat as they could be released and inhaled by the end-user, hindering the potential use of these composites as protective masks and clothing layers.[2,37]

To address these challenges, we developed an eco-benign aqueous phase growth method that enables the formation of a uniform coating of Zr-MOFs, including MOF-808 and UiO-66-NH_2, on the textile fiber without the need for chemical modification of the surface. We found that the use of trifluoroacetic acid (TFA) as the organic acid modulator is essential for this process and selectively confines MOF growth on the fiber surface rather than in the reaction media to generate unbonded particles.[37-38] The high acidity of TFA plays a key role in the slowdown of the MOF nucleation and growth to form localized coating on fiber surface, which acts as the inducer during MOF nucleation. Inductively coupled plasma optical emission spectroscopy (ICP-OES) studies show the mass loading of MOF are up to 20 wt%. We also demonstrated the generality of this method by successfully employing it with several common fibers, including polyester, polyacrylonitrile nanofiber, and polypropylene, which featured a range of surface properties and fibrous strands of different diameters. Finally, we illustrated the scalability of this method by synthesizing a MOF-808-coated PET composite that was one meter long.

1.2. Dip-coating method

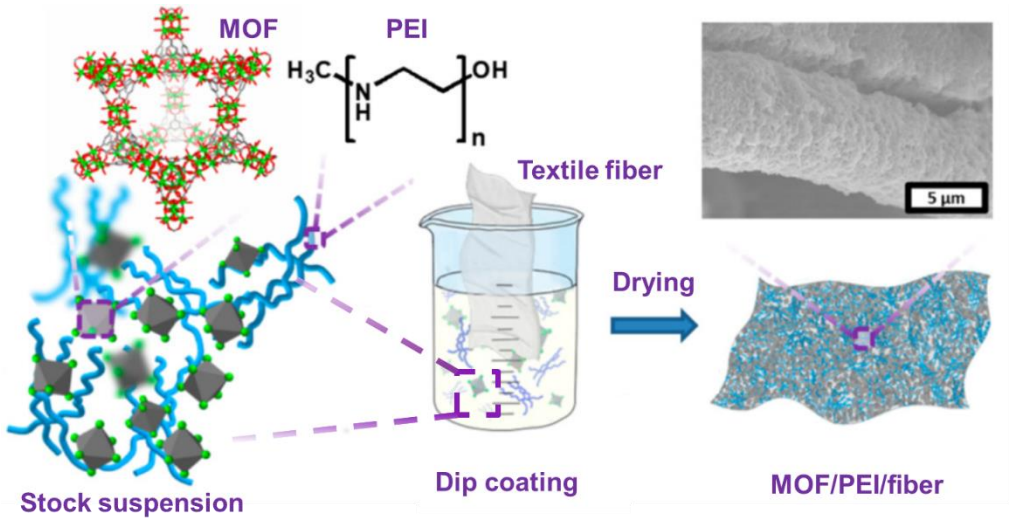

Figure 3. Schematic illustration of the dip-coating method using a stock solution of MOF and polymer. Adapted from ref (39). Copyright 2019 American Chemical Society.

The dip-coating method is widely used in industry to prepare functional coatings on textile surfaces. Recently, we extended this approach to prepare a highly uniform MOF-808/polyethylenimine (PEI)/textile composite by dipping a textile substrate into a stock suspension of MOF-808 nanoparticles and polymeric PEI in ethanol, which we then dried at room temperature.[39] ICP-OES testing indicates a MOF loading of 12 wt% in the composite. PEI serves as a binder that enhances the stability of coating. Moreover, the basicity of PEI greatly enhances the performance of this composite towards the catalytic hydrolysis of nerve agents (see Section 2.2). Notably, this strategy is amenable to the incorporation of different MOFs and polymers into the composite just by modifying the materials used in the stock suspension.

We then expanded on this approach and replaced the linear PEI in the MOF/fiber composite with a branched polyethylenimine hydrogel (BPEIH) to address kinetic limitations observed during the solid-state hydrolysis of nerve agents (see Section 2.2).[40] Cross-linking the branched PEI substrate with a diepoxide in an aqueous solution at room temperature afforded a hydrogel, which features a high density of amine groups and increased amount of adsorbed water due to the presence of hydroxy groups throughout the polymer. Dip-coating the PET substrate in an aqueous suspension of MOF-808 nanoparticles, branched PEI, and the diepoxide-based cross-linker, followed by incubating the composite at room temperature overnight afforded the MOF-808/hydrogel/PET composite with a MOF loading of 12 wt%.

We anticipate that this facile, room temperature dip-coating method could be extended to other kinds of MOF systems, such as Fe-, Al-, and other Zr-based MOFs, as well as onto a wide range of fibers, including thermally sensitive fibers. Moreover, this method

can likely be extended to commercial-scale production with the use of regular textile engineering equipment, such as roll-to-roll dip coating equipment, for the bulk production of functional protective clothing.

1.3. Biosynthesis method using bacteria

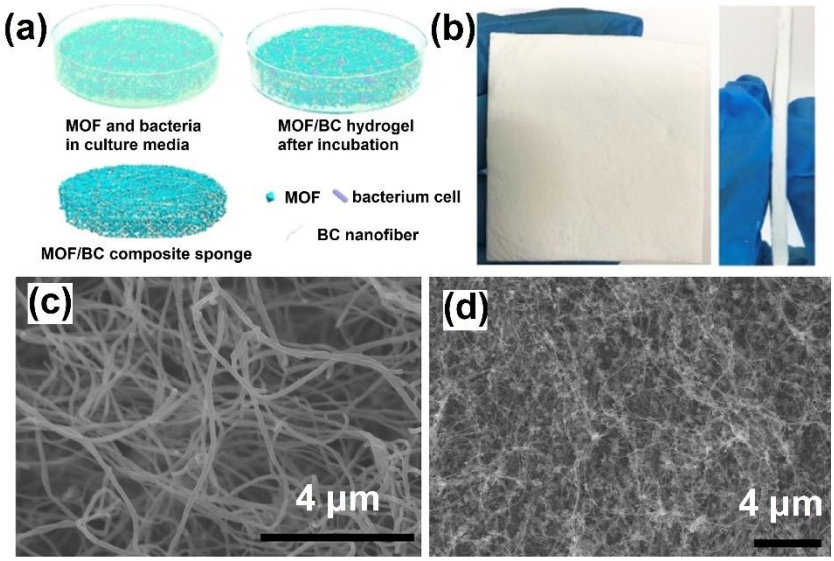

Figure 4. (a) Schematic illustration of the MOF/BC sponge biosynthesis. (b) Photograph of the MOF-808/BC composite sponge sample (6 cm×6 cm×0.3 cm). SEM images of (c) BC and (d) the MOF-808/BC composite sponge. Adapted with permission from ref (42). Copyright 2022 Wiley-VCH.

Building from our previous study into the MOF/PEI-based hydrogel composites, we considered other approaches that would enable access to low density, hydrogel-based fibrous composites. In particular, we envisioned that the hierarchical porosity and high mechanical and thermal stability of bacterial cellulose (BC), which is a biosynthesized fibrous nanocellulose, would generate a robust composite with accessible MOF particles. With this target in mind, our group pioneered a benign biosynthesis method to prepare MOF/cellulose composite sponges *via* fermentation of sugar in the presence of MOF nanoparticles (**Figure 4a**).[42] We employed the bio-safe *Gluconacetobacter xylinus (ATCC 23770),* which is used in food industry for vinegar production, as the fermentation strain to generate a BC network *in situ* as a substrate to support the MOF component. After incubation of bacteria with MOF nanoparticles in culture media containing sucrose, yeast extract, and peptone, we harvested a MOF/BC composite hydrogel, which we then activated to isolate a porous MOF-based sponge after removal of the solvent (**Figure 4b**). Importantly, this aqueous biosynthesis method avoids the use of toxic organic solvents, which may be trapped in the composite following the synthesis and pose a high risk to human health, improving the feasibility of this

composite to be used as a protective mask filter. The activated MOF-808/BC composite, which originated from the culture media with 40 mg mL^{-1}, 80 mg mL^{-1}, and 160 mg mL^{-1} MOF-808, were named MOF-808/BC-1, MOF-808/BC-2, and MOF-808/BC-3. ICP-OES studies show that the MOF mass loading in these three samples was 60 wt%, 75 wt%, and 90 wt%, respectively, indicating the mass loading in the composites is tunable. MOF/BC sponge achieves a MOF loading of up to ~90 wt%, which is among the highest loadings reported for similar composites, suggesting a high work capacity in toxin capture and detoxification.[42] The three-dimensional (3-D) hierarchical structure of the composite encourages substrate and product diffusion through the materials, which results in excellent catalytic activity towards the hydrolysis of nerve agent simulants (see Section 2.2). Finally, we immersed the activated MOF/BC sponge samples in refluxing dimethyl sulfoxide (DMSO), DMF, octane, or water for 24 h and observed no change in their crystallinity, porosity, or morphology, highlighting the robust nature of this BC-based composite.

2. MOF/fiber composite for chemical and biological protection

Chemical warfare agents, such as nerve agents and mustard gas, and biological risks, like pathogenic bacteria and viruses, pose serious threats to the public.[1-2] Traditional protective clothing and masks generally operate by physical adsorbing the chemical threat or by acting as a physical barrier from air. However, most of these passive protective materials suffer from low work capacities and cross infection or contamination following exposure to the threat. In this regard, functional MOF/fiber composites have shown great potential for both single-and multi-purpose protection.

2.1. Liquid-phase catalytic hydrolysis of chemical warfare agents and simulants

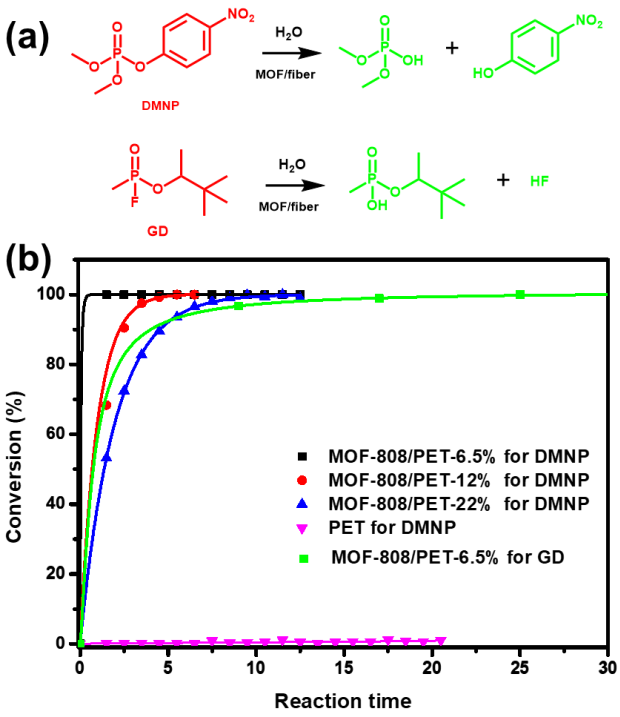

Figure 5. (a) Scheme for the catalytic hydrolysis of DMNP and GD. (b) Hydrolysis kinetics of DMNP and GD using MOF-808/PET as the catalyst. Conditions: 1.5 μmol MOF-808 in composite (corresponding to 6 mol % catalyst) and 25 μmol DMNP used in catalysis reaction. Adapted from ref (37). Copyright 2019 American Chemical Society.

Due to the presence of strongly Lewis-acidic Zr(IV) ions in their hexanuclear nodes, Zr-MOFs serve as excellent heterogeneous catalysts for the detoxification of organophosphorus nerve agents and their simulants. Generally, these reactions require basic conditions to displace the phosphonate or phosphate byproducts from the active sites at the Zr_6 nodes, allowing the reaction to proceed catalytically (Figure 5).[33] Initial studies from our group focused on improving the catalytic performance of Zr-MOFs in heterogeneous liquid-phase reactions (i.e., Zr-MOF powder suspended in a basic aqueous solution) until hydrolysis occurred almost instantly.[28,33] From here, we sought to translate this catalytic performance to MOF/fiber composites. First, we studied the catalytic performance of the *in situ* hydrothermally synthesized MOF-808/PET towards the hydrolysis of the nerve agent simulant dimethyl 4-nitrophenyl phosphonate (DMNP) in an aqueous solution with *N*-ethylmorpholine as the base (0.45 M, pH 10) (Figure 5a).[37] We found that varying the MOF loading in the composite affected the catalytic activity of the composite. For instance, when using two different composites with the same molar amount of MOF-808 (6 mol%) in catalysis, the initial half-lives of composites with 6.5 wt% and 22 wt% MOF-808 were about 0.5 and 3 min, respectively

(**Figure 5b**).[27] Since the catalytic loadings are normalized to the same amount of MOF-808 catalyst, the composite with the lower loading (6.5%) has relatively more external surface area that enhances substrate diffusion to the active sites, resulting in improved catalytic activity. Next, we explored the catalytic activity of the 6.5% MOF-808/fiber composite towards the real organophosphorus nerve agent O-pinacolyl methylphosphonofluoridate (GD) and observed a half-life of 2 min, which was the highest liquid-phase catalytic activity for a MOF composite towards the hydrolysis of GD reported at the time (**Figure 5b**).

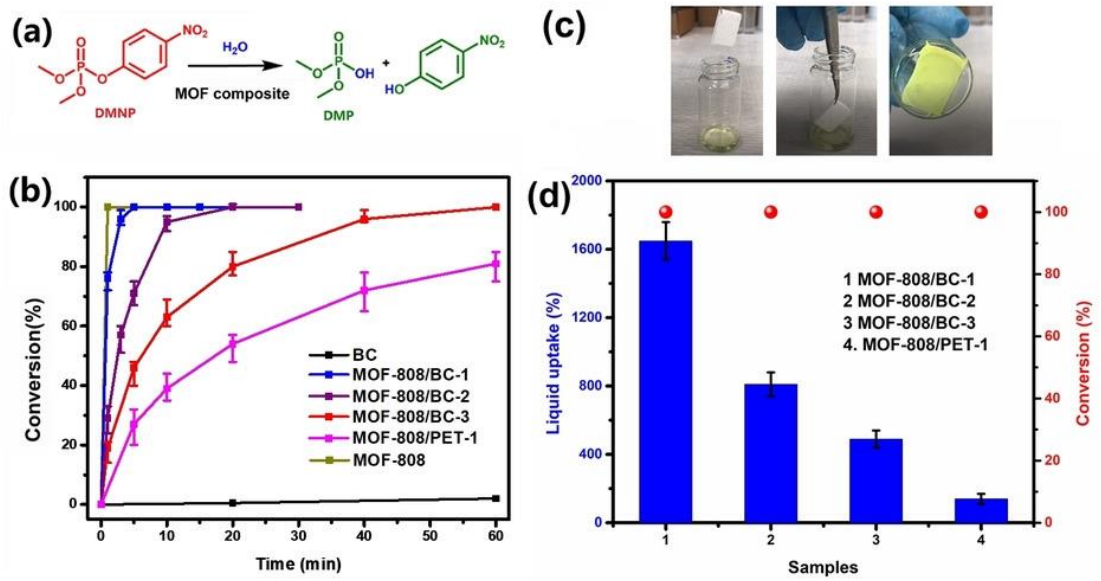

Figure 6. Hydrolysis of DMNP using the hierarchical MOF-808-BC composite sponge catalyst. (a) Liquid-phase hydrolysis kinetics of DMNP. Conditions: 1.5 μmol MOF-808 in composite (corresponding to 6 mol % catalyst) and 25 μmol DMNP used in the catalysis reaction. (b) Photographs showing the DMNP solution uptake using the MOF-808/BC composite sponge. (c) DMNP solution uptake percentage at 15 s and DMNP conversion at 2 min using different composites. (d) DMNP solution uptake percentage and conversion using different composites. Adapted with permission from ref (42). Copyright 2022 Wiley-VCH.

Building from these results, we hypothesized that a MOF/fiber composite structure with hierarchical porosity would improve substrate and product accessibility to the MOF-based active sites towards the interior of the composite, rather than be confined to the external active sites, and result in improved catalytic performance.[42] We studied the catalytic hydrolysis performance of the hierarchically porous MOF-808/BC-1 composite (50 wt% MOF loading) and the MOF-808/PET-1 composite (50 wt% MOF loading) towards DMNP under otherwise analogous conditions and found that the BC-based composite demonstrated a 20-fold increase in the hydrolysis kinetics with half-

lives of 1 min and 20 min, respectively (**Figure 6a**). These results emphasize how the greater substrate accessibility that results from the hierarchically porous composite structure improves the catalytic performance of the resulting composite compared to that of a non-porous composite structure. Therefore, the MOF-808/BC composite sponges are attractive for real applications due to the combination of highly accessible catalytic sites and high MOF loadings that afford high work capacities and improved catalytic activites.[42]

Given the hierarchical macro- and micro-porosity and the low density of the MOF-808/BC sponges, we explored their potential for simultaneously adsorbing and detoxifying DMNP from contaminated water (**Figure 6b,c**). MOF-808/BC-1 (about 50 wt% MOF loading) showed a liquid uptake 16 times the weight of contaminated water, while the relatively less macroporous MOF-808 coated commercial polyester cloth (MOF-808/PET -1, 50 wt% MOF loading) exhibited a liquid uptake of only 1.4 times the weight of contaminated water – an order of magnitude lower than that of the BC-based composite (**Figure 6d**). Squeezing the liquid from the composite to stop the catalytic reaction, ^{31}P NMR spectroscopic analysis indicates that MOF-808/BC sponges achieve full conversion of DMNP within 2 min (**Figure 6b,c**).[42] In addition, the MOF-808/BC sponges show good recyclability and stability against aging after storage on the benchtop for 4 months. Combined, these results indicate that these composite sponges are well-suited for the destruction of large stockpiles of nerve agents or for the fast remediation of environmental contamination by nerve agents.

Finally, we explored the use of MOF-808/fiber composites for the degradation and sensitive colorimetric detection of the nerve agent O-ethyl S-diisopropylaminoethyl methylphosphonothiolate (VX) by incorporating a reactive dye, ditopic 5,5-dithiobis (2-nitrobenzoic acid) (DTNB), into the MOF.[31] In this system, the Zr(IV)-based active sites serve to rapidly detoxify VX by selectively hydrolyzing its P-S bond, and the thiol byproduct reacts with the DTNB molecules coordinated to the node to produce a bright orange product. This color change for the MOF/fiber composite from white to orange is apparent enough to identify < 1 mg/cm^2 of VX on a contaminated surface, demonstrating the potential utility for this material in dual function sensing-detoxifying protection.

2.2. Solid-state hydrolysis of nerve agents

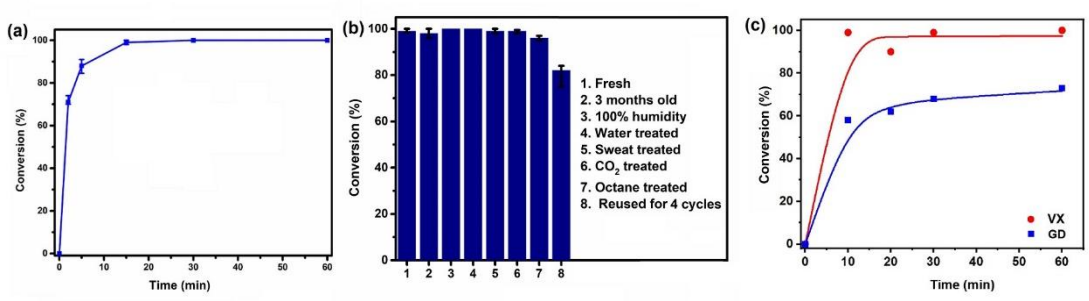

Figure 7. Solid state catalytic hydrolysis of nerve agents and simulants with the MOF-808/BPEIH/fiber composite. (a) Catalytic hydrolysis kinetics of the nerve agent simulant DMNP, (b) catalytic efficiency stability evaluation against different challenges during real world application, and (c) catalytic hydrolysis kinetics of the real nerve agents GD and VX. Adapted with permission from ref (40). Copyright 2021 Elsevier.

As described in the previous section (Section 2.1), these hydrolysis reactions require basic conditions to displace the tightly bound phosphonate or phosphate byproducts from the Zr_6 nodes, preventing deactivation of the MOF catalyst and allowing catalysis to proceed.[31,33,37] In liquid-phase reactions, researchers typically employ *N*-ethylmorpholine (NEM) as the base and perform these reactions in basic aqueous solutions at pH = 10. However, the high volatility of NEM and the requirement for bulk water hinder the potential implementation of these MOF/fiber composites as wearable protection gear under real-world conditions.

Targeting a system that would enable the practical solid-state detoxification of nerve agents under relevant conditions, our team developed the second-generation MOF/fiber protective clothing by replacing NEM with a heterogenized, nonvolatile polymeric base PEI.[39] Moreover, water molecules adsorbed to the MOF under ambient conditions could be utilized for hydrolysis, which would eliminate the need for bulk water in aqueous solutions. Following hydrolysis, PEI could regenerate the MOF catalytic sites to facilitate the solid-state hydrolysis under ambient humidity. When exposed to DMNP under 50% relative humidity, the MOF-808/PEI/fiber composite afforded an initial half-life of about 0.4 h. Notably, this is the first example of a fully solid-state system catalytically hydrolyzing organophosphorus substrates under atmospheric conditions. However, the hydrolysis kinetics for this system are much slower (half-lives XX min) than those of comparable liquid-phase reactions (half-lives < 1 min). We attributed this to the non-porous polymeric base providing a limited amount of OH^- species to regenerate the active sites under ambient humidity.

To further improve the regeneration efficiency of this solid-state Zr-MOF catalyst

system, we developed the third-generation active protective clothing in which we introduced a crosslinked branched polyethylenimine hydrogel (BPEIH) as the solid base, denoted as MOF-808/BPEIH/fiber (**Figure 7**; composite synthesis described in Section 1.2).[40] This composite features a high density of basic amine groups and an abundant supply of adsorbed water within the pores due to the presence of hydrophilic hydroxy and amine groups throughout the hydrogel. When exposed to DMNP under 50% relative humidity, the MOF-808/BEPIH/fiber composite yielded an initial half-life of 1 min and nearly quantitative conversion (99%) after 15 min, which is the highest reported catalytic activity for the fully solid-state hydrolysis of an organophosphorus nerve agent or simulant (**Figure 7a**).[40]

Importantly, the BPEIH-based protective MOF composites maintained their catalytic activity after storage on the bench top for several months and after exposure to challenging conditions, including high humidity, atmospheric CO_2, and commonly encountered contaminants (e.g., octane and perspiration), verifying the practicality of these composites for real-world protective applications (**Figure 7b**). Moreover, the MOF-808/BEPIH/fiber composite demonstrated the fastest kinetics to date in the fully solid-state hydrolysis of the real nerve agents VX and GD under ambient conditions with half-lives about 5 min and 10 min, respectively (**Figure 7c**).[40] The development of MOF-based protective clothing capable of performing rapid solid-state hydrolysis is a critical step toward effectively protecting both military personnel and civilians against CWA threats.

2.3. Selective Oxidation of Sulfur Mustards and Simulants

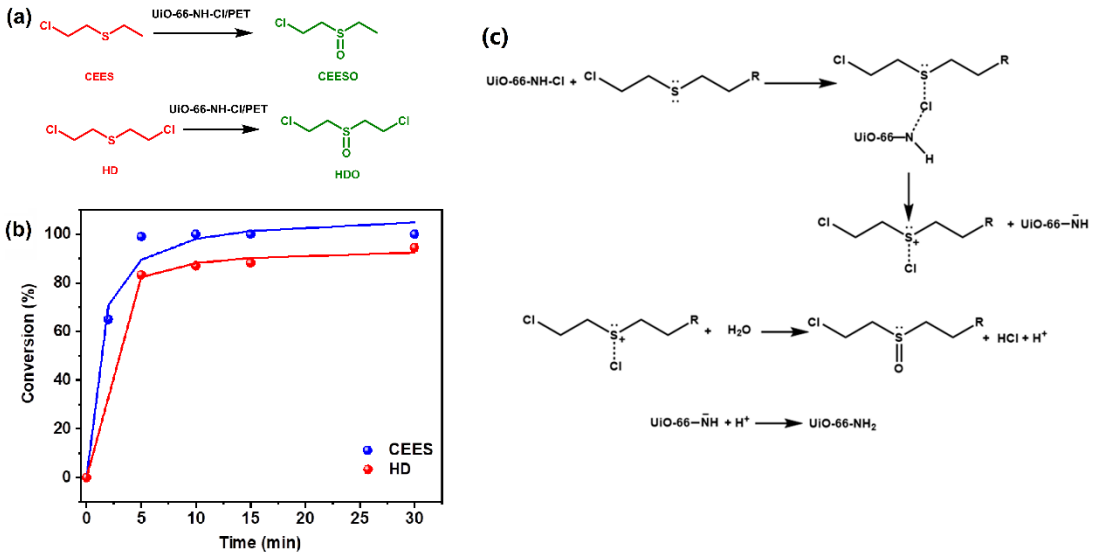

Figure 8. (a) Selective oxidation reaction of CEES and HD with the UiO-66-NH-Cl/PET composite. (b) Detoxification kinetics for both reactions. (c) A proposed selective oxidation mechanism of CEES or HD. R is CH_3 or Cl atom for CEES and HD, respectively. Adapted from ref (38). Copyright 2021 American Chemical Society.

Sulfur mustards, such as bis(2-chloroethyl) sulfide (mustard gas or HD) and its simulant 2-chloroethyl ethyl sulfide (CEES), comprise another dangerous class of CWAs that are less prone to hydrolysis than organophosphorus nerve agents, so they require alternative detoxification strategies. In particular, the oxidation of HD or CEES to the mono-oxidized sulfoxide product presents an attractive detoxification route, although the catalytic system must be selective for this transformation and limit over-oxidation to the highly toxic sulfone product (**Figure 8**). Recently, our group and others explored the catalytic photooxidation of both HD and CEES to the non-toxic sulfoxide compound using singlet oxygen generated upon irradiation of pyrene- or porphyrin-based MOF powders and their fibrous composites.[43] However, these methods require an LED light source to form reactive species and an organic solvent (e.g., methanol) to improve the selectivity for the desired sulfoxide product. For these systems to be implemented under practical conditions, the composite must selectively oxidize HD to the sulfoxide product in the absence of light, solvent, and other liquid reagents or oxidants.

With this goal in mind, we developed a composite based on an oxidative, *N*-chlorine-modified UiO-66-NH_2 coating that is capable of the solid-state detoxification mustard gas.[38] This oxidative composite, denoted as UiO-66-NH-Cl/PET, forms after a chlorine bleaching treatment of the pristine MOF-coated fiber composite and demonstrates the fast, selective oxidation of HD and CEES to the non-toxic sulfoxide products without the generation of the highly toxic sulfone product (**Figure 8a**). For example, treating the MOF/fiber composite with 3 equivalents of active chlorine species for affords a composite that can degrade HD and CEES with half-lives of only 3 min and 2 min, respectively **(Figure 8b)**. To the best of our knowledge, this is the first MOF/fiber composite that can rapidly and selectively detoxify HD in the absence of light or liquid reagents, paving the way for these composites to be used for the protection against sulfur mustards under practical conditions **(Figure 8c)**.[38]

2.4. Toxic chemical capture

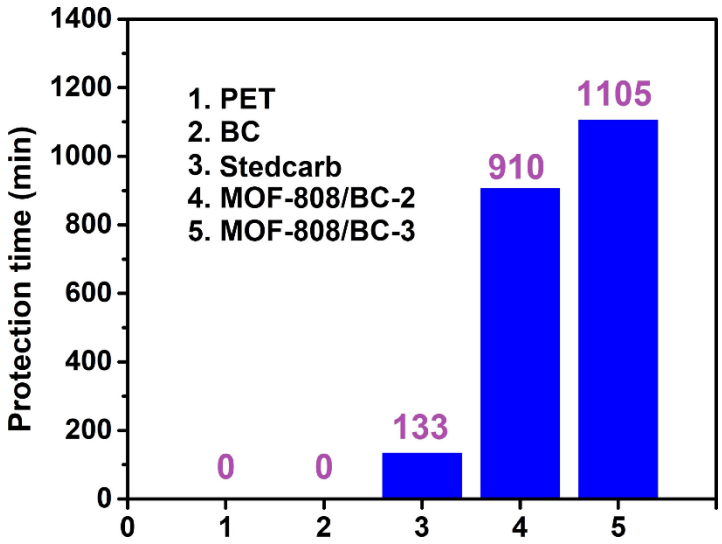

Figure 9. Protection time against nerve agent GD with different filter materials during a permeation testing, according to ASTM F739-12. Adapted with permission from ref (42). Copyright 2022 Wiley-VCH.

While improving catalytic performance of the composite offers one viable strategy to improve protection ability, designing composites that exhibit high retention times for CWAs could also improve performance by supplying more time for catalytic detoxification to occur, in addition to providing more protection by increasing the contact barrier from the human body.[42] To probe the permeation properties of these MOF/fiber composites against the real nerve agent GD, we employed a standard protocol (ASTM F739-12) for permeation evaluation of toxic gases through protective clothing materials under continuous contact conditions. Encouragingly, the bacterial cellulose-based MOF sponge composites described in Section 1.3, MOF-808/BC-2 (with 75 wt% MOF) and MOF-808/BC-3 (with 90 wt% MOF), provided a barrier against the total permeation of GD for 910 min and 1100 min, respectively, which correspond to 7- and 8.5-fold improvements compared traditional carbon cloth, Stedcarb, of the same thickness (**Figure 9**).[42] Furthermore, GD immediately fully permeates through both the commercial textile clothing and MOF-free bacterial cellulose sponge sample, excluding the capture capabilities of the fiber substrate without MOF incorporation. These results indicate that the MOF-based sponge composites are promising absorbent layers that can effectively decrease the diffusion rate of toxic chemicals through the protective cloth and reduce the harm to user. Moreover, the MOF-808 component does not only act as a porous absorbent, since it is also capable of hydrolyzing nerve agents, even in the absence of base. For example, dose extraction tests revealed that 98% of dosed GD hydrolyzed into non-toxic products after aging for 24 h, despite the absence of both liquid water and base. Combined, these

MOF-808/BC sponges demonstrate dual-function capture-degradation protection from nerve agents.[42] In addition, MOF-coated fibers can effectively capture the sulfur mustard simulant CEES from contaminated air flow, further illustrating the potential utility of this class of MOF-based composite materials.[37]

2.5. Biocidal applications

Since the outbreak of SARS-CoV-2 (COVID-19), the global community has sought an increasing amount of protective textiles, including masks, gowns, and other healthcare-related cloths, to mitigate risk of infection among the general population. However, significant demand for disposable protective textiles has strained global resources, and outbreak-related closures or operation suspensions of production facilities have posed additional challenges. Within healthcare settings, the long lifetime of the SARS-CoV-2 virus on contaminated surfaces and on the outer layer of surgical masks for up to seven days after exposure has highlighted the need for effective strategies to disinfect protective gear.[11-12] Due to this long lifetime, serious cross-infections have originated from protective textiles used in isolation centers, elderly homes, and hospitals.[10] The development of potent biocidal textiles would limit the chances for infection and better protect our communities from this virus.

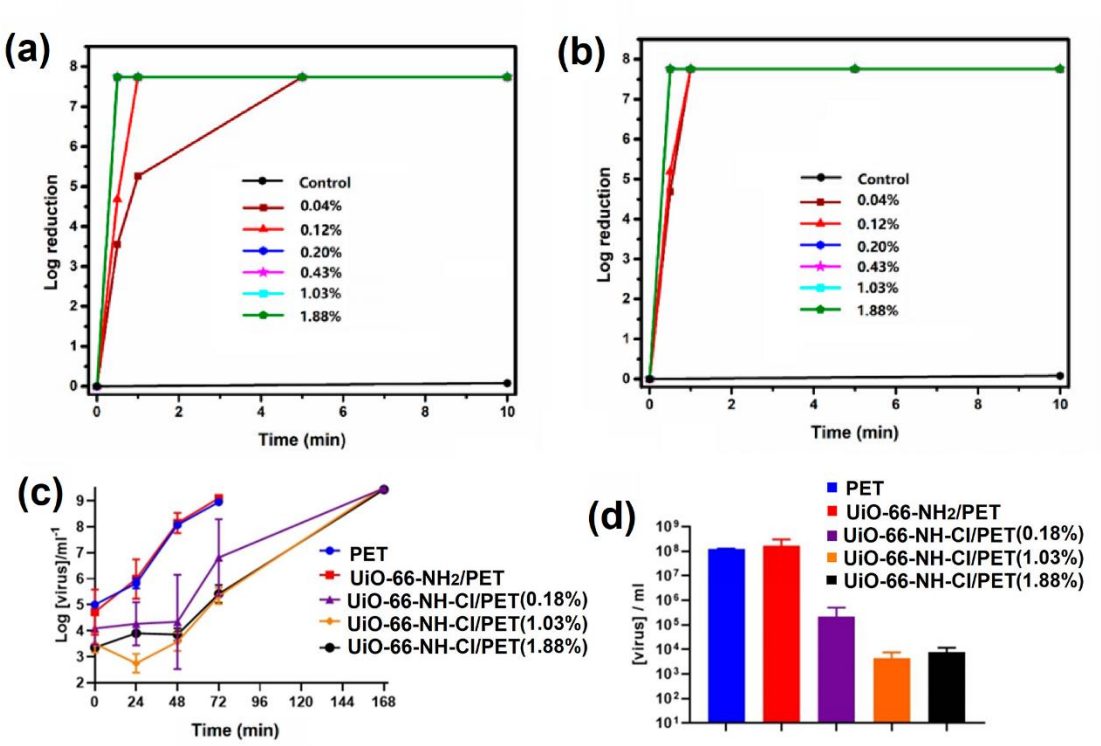

Figure 10. Antimicrobial activities of UiO-66-NH-Cl/PET with different active chlorine loadings against (a) *E. coli* and (b) *S. aureus*. (c) SARS-CoV-2 virus growth over time after treatment with the UiO-66-NH-Cl/PET composite. (d) SARS-CoV-2

titer differences at the 48 h time point. Adapted from ref (38). Copyright 2021 American Chemical Society.

Inspired by the wide use of chlorine bleach in both textile and environmental disinfection, we explored the biocidal activity of our active chlorine-loaded UiO-66-NH-Cl/PET composites. When exposed to Gram-negative bacterium and Gram-positive bacteria, the UiO-66-NH-Cl/PET composite demonstrates fast and broad-spectrum antibacterial activity with up to a 7-log reduction within 5 min (**Figure 10a,b**).[38] We further probed the biocidal activity of UiO-66-NH-Cl/PET against SARS-CoV-2, the pathogenic microorganism responsible for the global COVID-19 pandemic. The antivirus activities were determined by SARS-CoV-2 virus titers following virus exposure to the textile samples for 15 min (**Figure 10c,d**). Both the PET cloth and the MOF/PET without chlorination showed an immediate increase in virus titers and reached 10^8 mL^{-1} within 2 days, indicating rapid virus replication. In contrast, the chlorinated textiles showed a significant delay in virus growth (**Figure 10c,d**). The Real-time polymerase chain reaction (RT-qPCR) results indicate a log 3–5 reduction in virus titers after 48 h in the active cloth samples relative to those of the non-chlorinated control samples, emphasizing the effectiveness of this strategy **(Figure 10d)**.[38] Notably, we observed that achieving this chlorine loading on the UiO-66-NH_2 coating is repeatable for at least 5 consecutive cycles, demonstrating the excellent renewability of this composite and suggesting good reusability as a protective textile. This work highlights how UiO-66-NH-Cl/PET is a self-cleaning and reusable protective composite that can greatly reduce risk of virus exposure in healthcare settings.

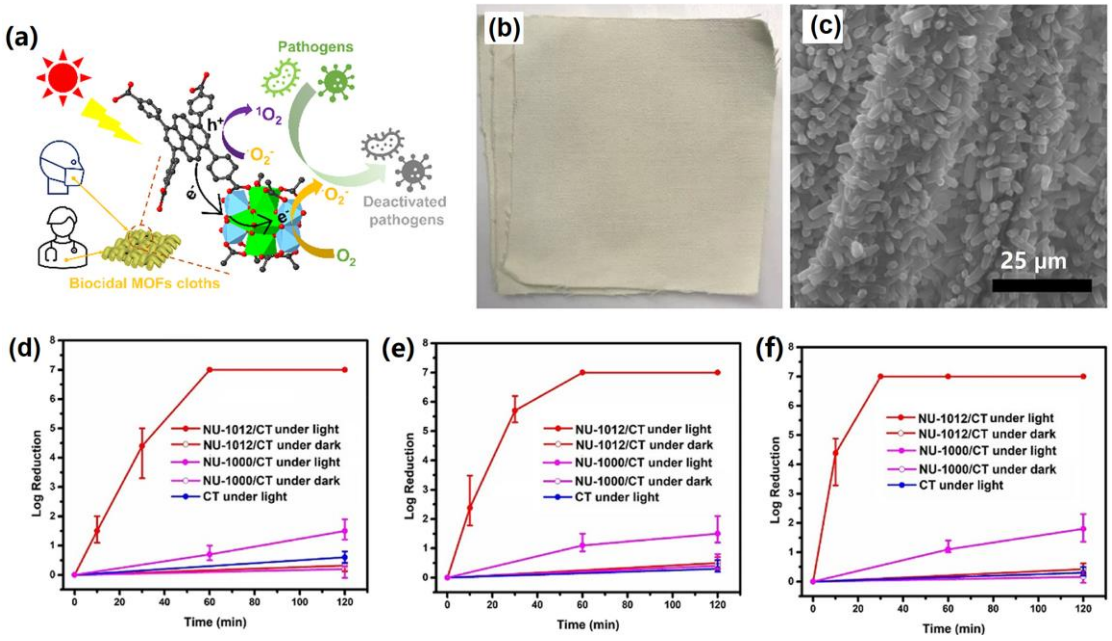

Figure 11. (a) Illustration of the photoactive biocidal NU-1012/CT and its mechanism

of pathogen deactivation. (b) Photographic image and (c) SEM image of the NU-1012/CT sample. Antipathogenic activities of cotton (CT), NU-1000/CT, and NU-1012/CT against (d) E. coli, (e) S. epidermidis, and (f) T7 phage. Adapted from ref (44). Copyright 2022 American Chemical Society.

In addition to the active chlorine loading-release strategy, we also developed a visible-light-induced biocidal coatings on fabrics using a photoactive MOF constructed with a titanium/zirconium cluster and a pyrene linker (**Figure 11 a**).[44] Post-synthetic metalation of the Zr-MOF NU-1000 with Ti affords a new Zr/Ti-MOF, NU-1012, following a rare linker migration phenomenon that generates the first example of a Zr_6Ti_4 node. We integrated NU-1012 onto cotton fibers (CT) by *in situ* growth to obtain NU-1012/CT composites (**Figure 11b-c**). Visible light irradiation causes electron transfer from the ligand to the mixed Zr/Ti-based node, which then produces reactive oxygen species (e.g., $^1O_2$ and $^{\bullet}O_2^-$) that are capable of oxidizing and deactivating pathogens. NU-1012/CT shows broad-spectrum antipathogenic performance against viruses, as well as Gram-positive and Gram-negative bacteria, within minutes under visible light irradiation (**Figure 11d-f**). Importantly, this proposed photoactive biocidal coating can be integrated to other types of surfaces in high-risk sites, such as hospitals and nursing homes, which may prevent infections from pathogenic infections.

3. Concluding Remarks and Prospects

In this Account, we summarized our recent advances in the design and synthesis of MOF/fiber composites and their application for human protection against chemical and biological risks. We presented three strategies for the straightforward fabrication of MOF/fiber composites, including the *in situ* hydrothermal growth of MOFs on fiber surfaces, the dip-coating of fibers into suspensions of pre-synthesized MOF particles, and a bio-synthesis method that incorporates pre-formed MOF particles into nanofiber networks generated *via* fermentation. The *in situ* growth method produce uniform and robust MOF coatings on fiber surfaces with good generality and tunable MOF loading. In comparison, the scalable dip-coating method enables the introduction of additional functional components, such as a polymeric base, into the MOF/fiber composite to afford practical protective clothing. These complementary strategies generate MOF/fiber composites that integrate the advantages of MOFs, such as catalytic reactivity and porosity, into flexible and protective textile materials.

Next, we illustrated the evolution of these composites into fully solid-state catalytic systems that can detoxify the nerve agent GD within minutes under ambient conditions. The key advance for this material involved the formation of a branched

polyethyleneimine-based hydrogel, which contains a large density of basic amine groups necessary to promote catalytic turnover, as well as water present at ambient humidity due to the hydrophilic hydroxy groups that enable hydrolysis to occur. Incorporating active chlorine species into MOF/fiber composites generates reactive textile materials that are not only capable of selectively oxidizing the sulfur mustard HD into the non-toxic sulfoxide product but can also deactivate pathogens within minutes of exposure. Finally, a composite containing a MOF built from mixed-metal Zr/Ti nodes and a pyrene-based linker exhibits biocidal activity upon visible light irradiation, paving the way towards the implementation of reactive, self-cleaning textile materials for use in healthcare settings.

Despite these significant recent advances in protective MOF/fiber composites, challenges remain in both material fabrication and application. First, further detailed studies are needed to better understand the mechanism and formation process of MOF coatings or films on fiber substrates, along with the interfacial interactions between MOF layers and the substrate surface. Second, industrial scale bulk production methods would boost the practical application of these materials, especially for roll-to-roll dip-coating techniques. Third, many reported MOF/fiber composites contain a single MOF layer on a fiber substrate, which may limit the use of these textiles to specific applications unless the MOF is versatile and capable of engaging in multiple modes of reactivity. Moving forward, the rational design of multi-component composites with more than one MOF and polymer could integrate multiple functionalities into one composite. Investigations into polybasic MOF/fiber composites towards protection from multiple risks will provide a more accurate description of the protection efficiency of these composites under relevant conditions. Moreover, the MOF/fiber composites could serve as bifunctional layers for both the capture and degradation of CWAs, and *in situ* studies into capture-detoxification performance should be explored using real CWAs to elucidate structure-property relationships. Furthermore, the rational design and overall hierarchical structure of MOF/fiber composites could be helpful to improve the protection activity by enabling better diffusion of substrates and products to the MOF-based active sites. Finally, the degradation of MOF components or leaching of MOF particles from the composite could hinder the application of these composites. Therefore, researchers should perform detailed investigations into how leached species degrade functionality and study their impact on human and environment safety.

Corresponding Authors

Kaikai Ma - International Institute for Nanotechnology, Institute for Sustainability and Energy at Northwestern, and Department of Chemistry, Northwestern University, 2145

Sheridan Road, Evanston, Illinois 60208, United States; https://orcid.org/0000-0003-0414-4397; Email: kaikai.ma@northwestern.edu

Omar K. Farha - International Institute for Nanotechnology, Institute for Sustainability and Energy at Northwestern, and Department of Chemistry, Northwestern University, 2145 Sheridan Road, Evanston, Illinois 60208, United States; Department of Chemical and Biological Engineering, Northwestern University, 2145 Sheridan Road, Evanston, Illinois 60208, United States; https://orcid.org/0000-0002-9904-9845; Email: o-farha@northwestern.edu

Author Contributions

[#]K.M, Y.H.C and K.O.K contributed equally to this work.

Notes

The authors declare the following competing financial interest(s): O.K.F. has a financial interest in the start-up company Nu-Mat Technologies, which is seeking to commercialize metal-organic frameworks.

ACKNOWLEDGMENTS

The authors acknowledge the financial support from the Army Research Office (W911NF1910340) and the Northwestern University Institute for Catalysis in Energy Processes (ICEP), funded by the DOE, Office of Basic Energy Sciences (Award Number DE-FG02- 03ER15457). This work made use of the J.B. Cohen X-ray Diffraction Facility supported by the MRSEC program of the National Science Foundation (DMR-1720139) at the Materials Re-search Center of Northwestern University. This work made use of Keck-II and EPIC facilities of the NUANCE Center at Northwestern University, which has received support from the Soft and Hybrid Nanotechnology Experimental (SHyNE) Resource (NSF NNCI-1542205); the MRSEC pro-gram (NSF DMR-1720139) at the Materials Research Center; the International Institute for Nanotechnology (IIN); the Keck Foundation; and the State of Illinois, through the IIN. This work made use of the IMSERC at Northwestern University, which has received support from the NSF (CHE-1048773 and DMR-0521267); the State of

Illinois and IIN. K.O.K. gratefully acknowledges support from the IIN Postdoctoral Fellowship and the Northwestern University International Institute for Nanotechnology. J.H.X. acknowledges the support from General Research Fund of the Research Grants Council of the Hong Kong SAR Government (GRF 15208420).

Reference

1. Jabbour, C.R.; Parker, L.A.; Hutter, E.M.; and Weckhuysen, B. Chemical targets to deactivate biological and chemical toxins using surfaces and fabrics. *Nat. Rev. Chem.* ***2021****, 5, 370–387.*
2. Peterson, G.; Lee, D.T.; Barton, H.F.; Epps, T.H.; and Parsons, G. Fibre-based composites from the integration of metal–organic frameworks and polymers. *Nat. Rev. Mater.* ***2021****, 6,* 605–621.
3. Melander, R. J.; Melander, C., The Challenge of overcoming antibiotic resistance: an adjuvant approach? *ACS Infect. Dis.* **2017,** *3* (8), 559-563.
4. Metcalf, C. J. E.; Lessler, J., Opportunities and challenges in modeling emerging infectious diseases. *Science* **2017,** *357* (6347), 149-152.
5. Sohrabi, C.; Alsafi, Z.; O'Neill, N.; Khan, M.; Kerwan, A.; Al-Jabir, A.; Iosifidis, C.; Agha, R., World Health Organization declares global emergency: A review of the 2019 novel coronavirus (COVID-19). *Int. J. Surg.* **2020,** *76*, 71-76.
6. Cheng, V. C.-C.; Wong, S.-C.; Chuang, V. W.-M.; So, S. Y.-C.; Chen, J. H.-K.; Sridhar, S.; To, K. K.-W.; Chan, J. F.-W.; Hung, I. F.-N.; Ho, P.-L.; Yuen, K.-Y., The role of community-wide wearing of face mask for control of coronavirus disease 2019 (COVID-19) epidemic due to SARS-CoV-2. *J. Infect.* **2020,** *81* (1), 107-114.
7. Eikenberry, S. E.; Mancuso, M.; Iboi, E.; Phan, T.; Eikenberry, K.; Kuang, Y.; Kostelich, E.; Gumel, A. B., To mask or not to mask: Modeling the potential for face mask use by the general public to curtail the COVID-19 pandemic. *Infect. Dis. Model.* **2020,** *5*, 293-308.
8. Leung, C. C.; Lam, T. H.; Cheng, K. K. J. L., Mass masking in the COVID-19 epidemic: people need guidance. *Lancet* **2020,** *395* (10228), 945.
9. World Health Organization. Coronavirus disease (COVID-19) advice for the public: when and how to use masks. Available at https://www.who.int/emergencies/diseases/novel-coronavirus-2019/advice-for-public/when-and-how-to-use-masks. Accessed May 09, 2022.
10. Koca, O.; Altoparlak, U.; Ayyildiz, A.; Kaynar, H., Persistence of nosocomial pathogens on various fabrics. *Eurasian J. Med.* **2012,** *44* (1), 28-31.
11. Chin, A. W. H.; Chu, J. T. S.; Perera, M. R. A.; Hui, K. P. Y.; Yen, H.-L.; Chan, M. C. W.; Peiris, M.; Poon, L. L. M., Stability of SARS-CoV-2 in different environmental conditions. *The Lancet Microbe* **2020,** *1* (1), e10.

12. van Doremalen, N.; Bushmaker, T.; Morris, D. H.; Holbrook, M. G.; Gamble, A.; Williamson, B. N.; Tamin, A.; Harcourt, J. L.; Thornburg, N. J.; Gerber, S. I.; Lloyd-Smith, J. O.; de Wit, E.; Munster, V. J., Aerosol and surface stability of SARS-CoV-2 as compared with SARS-CoV-1. *N. Engl. J. Med.* **2020,** *382* (16), 1564-1567.
13. Islamoglu, T.; Chen, Z.; Wasson, M. C.; Buru, C. T.; Kirlikovali, K. O.; Afrin, U.; Mian, M. R.; Farha, O. K. Metal−organic frameworks against toxic chemicals. *Chem. Rev.* **2020**, *120*, 8130-8160.
14. Furukawa, Kitagawa, S.; Kitaura, R.; Noro, S.-i. Functional Porous Coordination Polymers. *Angew. Chem., Int. Ed.* **2004**, *43*, 2334−2375.
15. Li, H.; Eddaoudi, M.; O'Keeffe, M.; Yaghi, O. M., Design and synthesis of an exceptionally stable and highly porous metal-organic framework. *Nature* **1999,** *402* (6759), 276-279.
16. Li, M.; Li, D.; O'Keeffe, M.; Yaghi, O. M., Topological Analysis of Metal–organic frameworks with polytopic linkers and/or multiple building units and the minimal transitivity principle. *Chem. Rev.* **2014,** *114* (2), 1343-1370.
17. Serre, C.; Mellot-Draznieks, C.; Surblé, S.; Audebrand, N.; Filinchuk, Y.; Férey, G. Role of Solvent-Host Interactions That Lead to Very Large Swelling of Hybrid Frameworks. *Science* **2007**, *315*, 1828.
18. Denny, M. S., Jr.; Moreton, J. C.; Benz, L.; Cohen, S. M. Metal−organic frameworks for membrane-based separations. *Nat. Rev. Mater.* 2016, *1*, 16078−16085.
19. Barea, E.; Montoro, C.; Navarro, J. A. Toxic gas removal − metal−organic frameworks for the capture and degradation of toxic gases and vapours. *Chem. Soc. Rev.* **2014**, *43*, 5419−5430.
20. Kitao, T.; Zhang, Y.; Kitagawa, S.; Wang, B.; Uemura, T. Hybridization of MOFs and polymers. *Chem. Soc. Rev.* **2017**, *46*, 3108−3133.
21. Wasson, M. C.; Buru, C. T.; Chen, Z.; Islamoglu, T.; Farha, O. K. Metal−organic frameworks: a tunable platform to access single site heterogeneous catalysts. *Appl. Catal. A* **2019**, *586*, 117214.
22. DeCoste, J. B.; Peterson, G. W. Metal-organic frameworks for air purification of toxic chemicals. *Chem. Rev.* **2014**, *114*, 5695−5727.
23. Zhao, J.; Lee, D. T.; Yaga, R. W.; Hall, M. G.; Barton, H. F.; Woodward, I. R.; Oldham, C. J.; Walls, H. J.; Peterson, G. W.; Parsons, G. N. Ultra-fast degradation of chemical warfare agents using MOF-nanofiber kebabs. *Angew. Chem., Int. Ed.* **2016**, *55*, 13224−13228.
24. Kalaj, M.; Cohen, S. M. Spray-coating of catalytically active MOF−polythiourea through postsynthetic polymerization. *Angew. Chem., Int. Ed.* **2020**, *59*, 13984−13989.
25. Wang, H.; Mahle, J. J.; Tovar, T. M.; Peterson, G. W.; Hall, M. G.; DeCoste, J. B.; Buchanan, J. H.; Karwacki, C. J. Solid-phase detoxification of chemical warfare

agents using zirconium-based metal organic frameworks and the moisture effects: analyze via digestion. *ACS Appl. Mater. Interfaces* **2019**, *11*, 21109−21116.

26. Moon, S.-Y.; Liu, Y.; Hupp, J. T.; Farha, O. K. Instantaneous Hydrolysis of Nerve-Agent Simulants with a Six-Connected Zirconium-Based Metal-Organic Framework. *Angew. Chem., Int. Ed.* **2015**, 54, 6795−6799.
27. Li, P.; Li, J.; Feng, X.; Li, J.; Hao, Y.; Zhang, J.; Wang, H.; Yin, A.; Zhou, J.; Ma, X.; and Wang, B. Metal-organic frameworks with photocatalytic bactericidal activity for integrated air cleaning. *Nat. Commun.* ***2019****, 10,* 2177.
28. Zhang, B.; Chen, H.W.; Hu, Q.H.; Jiang, L.M.; Shen, Y.Q.; Zhao, D.; Zhou, Z.X. CelluMOFs: Green, facile, and flexible metal-organic frameworks for versatile applications. *Adv. Funct. Mater.*, **2021**,*31*, 2105395.
29. López-Maya, E.; Montoro, C.; Rodríguez-Albelo, L. M.; Aznar Cervantes, S. D.; Lozano-Pérez, A. A.; Cenís, J. L.; Barea, E.; Navarro, J. A. R., Textile/Metal–organic-framework composites as self-detoxifying filters for chemical-warfare agents. *Angew. Chem. Int. Ed.* **2015,** *54* (23), 6790-6794.
30. Zhang, Y.; Yuan, S.; Feng, X.; Li, H.; Zhou, J.; Wang, B., Preparation of nanofibrous metal–organic framework filters for efficient air pollution control. *J. Am. Chem. Soc.* **2016,** *138* (18), 5785-5788.
31. Kirlikovali, K. O.; Chen, Z. J.; Islamoglu, T.; Hupp, J. T.; Farha, O. K. Zirconium-Based Metal-Organic Frameworks for the Catalytic Hydrolysis of Organophosphorus Nerve Agents. A*CS Appl. Mater. Interfaces* **2020**, 12, 14702−14720
32. Cao, R.; Chen, Z.; Chen, Y.; Idrees, K. B.; Hanna, S. L.; Wang, X.; Goetjen, T. A.; Sun, Q.; Islamoglu, T.; Farha, O. K. Benign Integration of a Zn-Azolate Metal−Organic Framework onto Textile Fiber for Ammonia Capture. *ACS Appl. Mater. Interfaces* **2020**, *12*, 47747−47753.
33. Ma, X.; Chai, Y.; Li, P.; Wang, B. Metal–organic framework films and their potential applications in environmental pollution control. *Acc. Chem. Res.* **2019***, 52*, 1461–1470.
34. Ma, K.; Idrees, K. B.; Son, F. A.; Maldonado, R.; Wasson, M.C.; Zhang, X.; Wang, X.; Shehayeb, E.; Merhi, A.; Kaafarani, B. R.; Timur Islamoglu, T.; John H. Xin, J. H.; Farha, O. K. Fiber composites of metal−organic frameworks. *Chem. Mater.***2020***, 32*, 7120−7140.
35. Ma, K.; Islamoglu, T.; Chen, Z.; Li, P.; Wasson, M. C.; Chen, Y.; Wang, Y.; Peterson, G. W.; Xin, J. H.; Farha, O. K. Scalable and template-free aqueous synthesis of zirconium-based metal–organic framework coating on textile fiber. *J. Am. Chem. Soc.* **2019**, *141*, 15626–15633.
36. Cheung, Y. H.; Ma, K.; van Leeuwen, H. C.; Wasson, M. C.; Wang, X.; Idrees, K. B.; Gong, W.; Cao, R.; Mahle, J. J.; Islamoglu, T.; Peterson, G. W.; de Koning, M. C.; Xin, J. H.; Farha, O. K., Immobilized regenerable active chlorine within a zirconium-based MOF

textile composite to eliminate biological and chemical threats. *J. Am. Chem. Soc.* **2021,** *143* (40), 16777-16785.

37. Chen, Z.; Ma, K.; Mahle, J.J..; Wang, H.; Syed, Z.H.; Atilgan, A.; Chen, Y.; Xin, J. H.; Peterson, G. W.; Islamoglu, T.; Peterson, G. W.; Farha, O. K. Integration of metal-organic frameworks on protective layers for destruction of nerve agents under relevant conditions. *J. Am. Chem. Soc.* **2019**, 141, 20016–20021.
38. Ma, K.; Wasson, M. C.; Wang, X.; Zhang, X.; Idrees, K. B.; Chen, Z.; Wu, Y.; Lee, S.; Cao, R.; Chen, Y.; Yang, L.; Son, F.A.; Islamoglu, T.; Peterson, G. W.; Mahle, J. J.; Farha, O. K. Near-instantaneous catalytic hydrolysis of organophosphorus nerve agents with zirconium-based metal–organic framework hydrogel composites. *Chem Catalysis.* **2021**, *1,* 1-13.
39. de Koning, M. C.; Ma, K.; van Grol, M.; Iordanov, I.; Kruijne, M. J. L.; Idrees, K. B.; Xie, H.; Islamoglu, T.; Bross, R. P. T.; Farha, O. K. Development of a Metal–Organic Framework/Textile Composite for the Rapid Degradation and Sensitive Detection of the Nerve Agent VX. *Chem. Mater* **2022**, *34*, 1269– 1277.
40. Cheung, Y. H.; Ma, K.; Wasson, M. C.; Wang, X.; Idrees, K. B.; Islamoglu, T.; Mahle, J.; Peterson, G. W.; Xin, J. H.; Farha, O. K. Environmentally Benign Biosynthesis of Hierarchical MOF/Bacterial Cellulose Composite Sponge for Nerve Agent Protection. *Angew. Chem., Int. Ed.* **2022**, 8, e202202207.
41. Lee, D. T.; Jamir, J. D.; Peterson, G.; Parsons, G. Protective fabrics: metal-organic framework textiles for rapid photocatalytic sulfur mustard simulant detoxification. *Matter* **2020**, *2*, 404–415.
42. Wang, X.; Ma, K.; Goh, T.; M., Xie, H.; Mao, H.; Duan, J.; Kirlikovali, K.; Stone, A.; Ray, D.; Wasielewski, M.; Gagliardi, L.; Farha, O.K. Photocatalytic Biocidal Coatings Featuring Zr_6Ti_4-Based Metal−Organic Frameworks, *J. Am. Chem. Soc.* **2022**, 144, 12192–12201.